

Electronic Supplementary Information (ESI)

Highly augmented, (12,3)-connected Zr-MOF containing hydrated coordination sites for the catalytic transformation of gaseous CO₂ to cyclic carbonates

Guanghua Jin,^{‡a} Debobroto Sensharma,^{‡a} Nianyong Zhu,^a Sebastien Vaesen^a and Wolfgang Schmitt^{a,*}

^aSchool of Chemistry and AMBER centre, Trinity College Dublin, College Green, Dublin 2, Ireland. E-mail: schmittw@tcd.ie; Fax: +353-1-6712826; Tel: +353-1-8963495

[‡] Authors contributed equally

-
- S1. Materials and MOF Syntheses
 - S2. Physicochemical Characterisation and Methods
 - S3. Gas Sorption Analysis
 - S4. Single Crystal X-ray Diffraction and Structural Analysis
 - S5. Topological Reduction
 - S6. Catalysis
 - S7. References

S1. Materials and MOF Syntheses

Materials

All commercial available chemicals were used as obtained in high purity and from standard chemical suppliers without further purification. The 4,4',4''-[1,3,5-benzenetriyltris(ethyne-2,1-diyl)]tribenzoic acid (H₃bteb) ligand was prepared using a modified literature procedure.⁵¹

Synthesis of [Zr₆(BTEB)₄(μ₃-O)₄(μ₃-OH)₄(H₂O)₄] (TCM-16)

[Zr₆(BTEB)₄(μ₃-O)₄(μ₃-OH)₄(H₂O)₄] was synthesised by dissolving 28.8 mg of ZrCl₄ (0.12 mmol), 46.4 mg of H₃BTEB (0.09 mmol), and 1.465 g (12 mmol) of benzoic acid in 8 mL of dimethylformamide (DMF) in a closed vial and heating the reaction mixture to 120 °C for four days. Colourless crystals of [Zr₆(BTEB)₄(μ₃-O)₄(μ₃-OH)₄(H₂O)₄]:solv were obtained, washed with acetone and stored at ambient conditions. Yield: 31 mg, ca. 55 % based on Zr. Microanalytical data for C₁₃₂H₇₂O₃₆Zr₆ (including additional 9.5 H₂O and 0.5 DMF solvent molecules), calc (%): C 53.64, H 3.19, N: 0.23; found: C 53.46, H 2.64, N 0.15.

S2. Physicochemical Characterisation and Methods

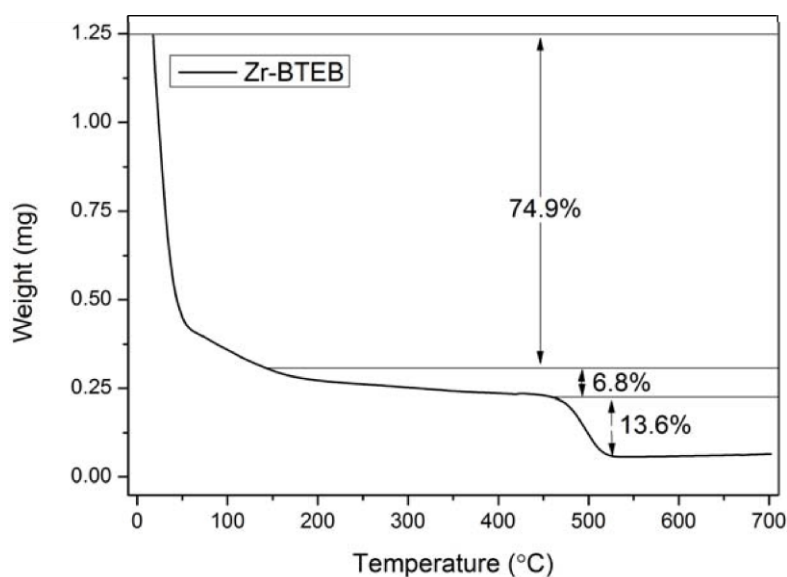


Figure S1: Thermogravimetric analysis of TCM-16 under a N₂ stream.

Thermogravimetric analysis (TGA) was carried out using a Perkin Elmer Pyris-1 thermogravimetric analyser under a continuous flow of nitrogen. Data collection was carried out between 20 °C and 700 °C at a heating rate of 5 °C per minute.

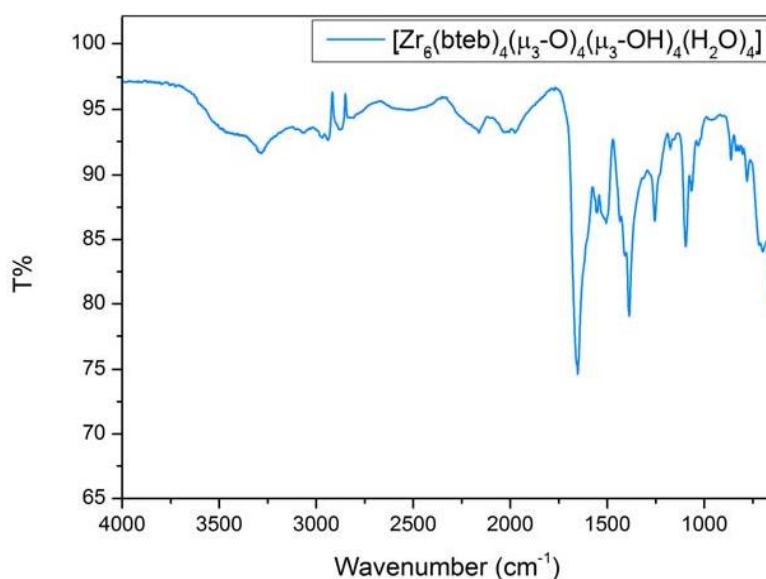


Figure S2: ATR-FTIR spectrum of TCM-16.

Infrared spectroscopy was conducted using a PerkinElmer Spectrum One FT-IR spectrometer using a universal ATR sampling accessory. Data was collected and processed using Spectrum v5.0.1 (2002 PerkinElmer Instrument LLC) software. 16 scans were collected in the range 4000-650 cm^{-1} .

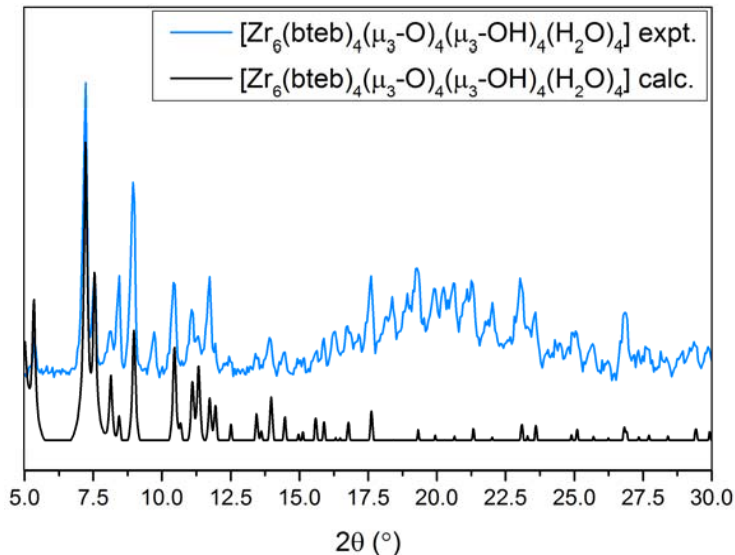


Figure S3: Experimental powder X-ray pattern of TCM-16, plotted against the calculated pattern from the single crystal X-ray structural model. The signal at ca. $2\theta = 9^\circ$ may derive from the use of excess benzoic acid in the synthesis which can result in ligand replacement at the hexanuclear SBU.

Powder X-ray diffraction data were collected at 293 K on a Bruker D2 Phaser diffractometer which employed a sealed tube Cu X-ray source (wavelength = 1.5406 Å), operating at 30 kV and 10 mA, and LynxEye PSD detector in Bragg-Brentano geometry at 2θ values from 5 to 55 degrees in a 60 minute scan.

S3. Gas Sorption Analysis

The adsorption measurements were performed on a Quantachrome Autosorb-iQ. The temperature was maintained at 278, 293, and 308 K using a circulating Dewar and a refrigerated/heated bath circulator (ISOTEMP 4100 R20 provided by Fischer Scientific), and at 77 K using a liquid nitrogen bath. The sample was activated at 353 K for 12 hours under secondary vacuum prior to the measurements and the mass of the sample was measured after the activation. The N₂, He and CO₂ gases cylinder in CP grade are provided by BOC Gases Ireland.

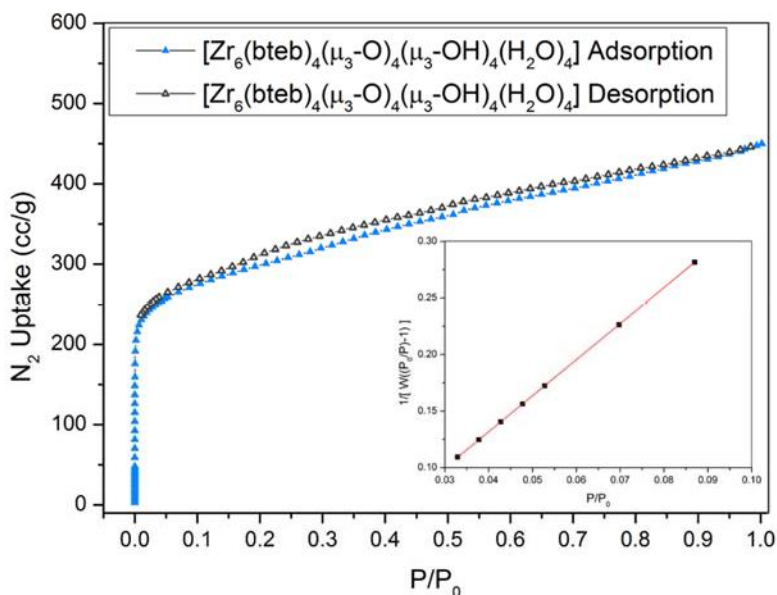


Figure S4: N₂ sorption isotherm of TCM-16 at 77 K.

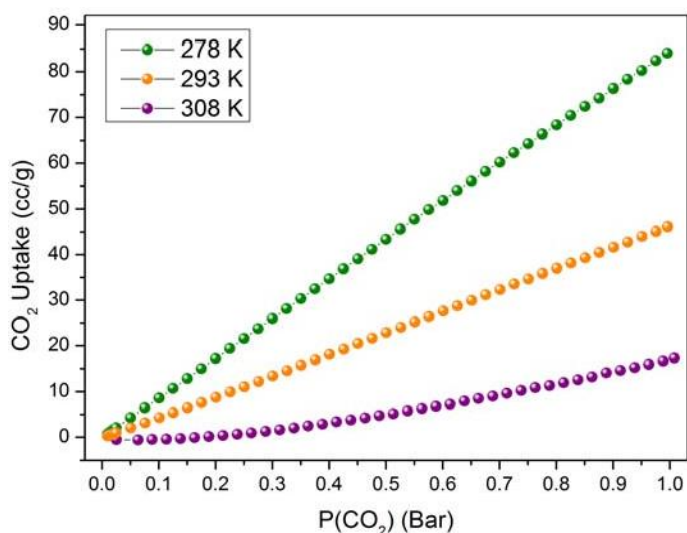


Figure S5: CO₂ adsorption isotherms of TCM-16 at 278 K, 293 K, and 308 K.

S4. Single Crystal X-ray Diffraction and Structural Analysis

A single crystal was mounted in a glass capillary containing a small amount of DMF. Data were collected on a Bruker APEX II DUO CCD diffractometer equipped with a $1\mu\text{S Cu K}\alpha$ microfocus tube (wavelength of 1.54184 Å). The single crystal was cooled to 215 K, using an Oxford Cryostream low-temperature device. The diffraction frames were integrated and processed using the Bruker SAINT software package. The data were corrected for absorption effects using the multi-scan method (SADABS).⁵² The structure was solved using SHELXT and refined using the SHELXL routine.⁵³ The positional and anisotropic displacement parameters for the non-hydrogen atoms were refined. Hydrogen atoms were constrained to idealized geometries and allowed to ride on their carrier atoms with an isotropic displacement parameter related to the equivalent displacement parameter of their carrier atoms. The structure contains large solvent accessible void volume in which solvent molecules could not be located reliably. To account for this, the Platon-SQUEEZE routine was used to calculate the void volume and re-generate the reflection file by excluding the diffraction contributions of these unlocated solvent molecules. The final results are based on the new reflection data.⁵⁴

Crystallographic data (**CCDC No. 1916002**) can be obtained free of charge from the Cambridge Crystallographic Data Centre via www.ccdc.cam.ac.uk/data_request/cif. Crystal data and structure refinement details are summarised in Table S1.

Table S1: Crystal data and structure refinement for TCM-16.

Identification code	TCM-16	
Empirical formula	$C_{222}H_{282}N_{30}O_{66}Zr_6$	
Formula weight	4974.08 g mol ⁻¹	
Temperature	215(2) K	
Wavelength	1.54184 Å	
Crystal system	Tetragonal	
Space group	<i>I</i> 4/ <i>m</i>	
Unit cell dimensions	$a = 33.102(3)$ Å	$\alpha = 90^\circ$
	$b = 33.102(3)$ Å	$\beta = 90^\circ$
	$c = 21.711(2)$ Å	$\gamma = 90^\circ$
Volume	23790(5) Å ³	
Z	2	
Density (calculated)	0.694 Mg/m ³	
Absorption coefficient	1.406 mm ⁻¹	
F(000)	5184	
Crystal size	0.24 x 0.1 x 0.1 mm ³	
Theta range for data collection	2.434 to 45.813°.	
Index ranges	-30 ≤ h ≤ 30, -26 ≤ k ≤ 30, -20 ≤ l ≤ 19	
Reflections collected	39877	
Independent reflections	5175 [R(int) = 0.0638]	
Completeness to theta = 45.813°	99.6 %	
Absorption correction	Semi-empirical from equivalents	
Max. and min. transmission	0.7490 and 0.2276	
Refinement method	Full-matrix least-squares on F ²	
Data / restraints / parameters	5175 / 146 / 220	
Goodness-of-fit on F ²	1.066	
Final R indices [I > 2σ(I)]	R1 = 0.0577, wR2 = 0.1643	
R indices (all data)	R1 = 0.0749, wR2 = 0.1762	
Extinction coefficient	n/a	
Largest diff. peak and hole	0.491 and -0.801 e.Å ⁻³	

S5. Topological Reduction

Topology for ZA1

Atom ZA1 links by bridge ligands and has

Common vertex with				R(A-A)		
ZB 1	1.0000	1.0000	0.5000	(1 0 0)	13.910A	1
ZB 1	0.5000	0.5000	1.0000	(0 0 1)	14.514A	1
ZB 1	0.5000	0.5000	0.0000	(0 0 0)	14.514A	1

Topology for ZB1

Atom ZB1 links by bridge ligands and has

Common vertex with				R(A-A)		
ZA 1	0.2307	0.1775	0.0000	(-1-1 0)	13.910A	1
ZA 1	0.1775	0.7693	0.0000	(-1 1 0)	13.910A	1
ZA 1	0.8225	0.2307	0.0000	(1-1 0)	13.910A	1
ZA 1	0.7693	0.8225	0.0000	(1 1 0)	13.910A	1
ZA 1	0.3225	0.7307	-0.5000	(1 0-1)	14.514A	1
ZA 1	0.3225	0.7307	0.5000	(1 0 0)	14.514A	1
ZA 1	0.6775	0.2693	-0.5000	(0 1-1)	14.514A	1
ZA 1	0.6775	0.2693	0.5000	(0 1 0)	14.514A	1
ZA 1	0.2693	0.3225	-0.5000	(1 1-1)	14.514A	1
ZA 1	0.2693	0.3225	0.5000	(1 1 0)	14.514A	1
ZA 1	0.7307	0.6775	0.5000	(0 0 0)	14.514A	1
ZA 1	0.7307	0.6775	-0.5000	(0 0-1)	14.514A	1

Structural group analysis

Structural group No 1

Structure consists of 3D framework with ZBZA4

Coordination sequences

ZA1: 1 2 3 4 5 6 7 8 9 10
Num 3 28 19 126 51 286 99 510 163 798
Cum 4 32 51 177 228 514 613 1123 1286 2084

ZB1: 1 2 3 4 5 6 7 8 9 10
Num 12 10 76 34 204 74 396 130 652 202
Cum 13 23 99 133 337 411 807 937 1589 1791

TD10=2025

Vertex symbols for selected sublattice

ZA1 Point symbol:{4^3}
Extended point symbol:[4.4.4(3)]

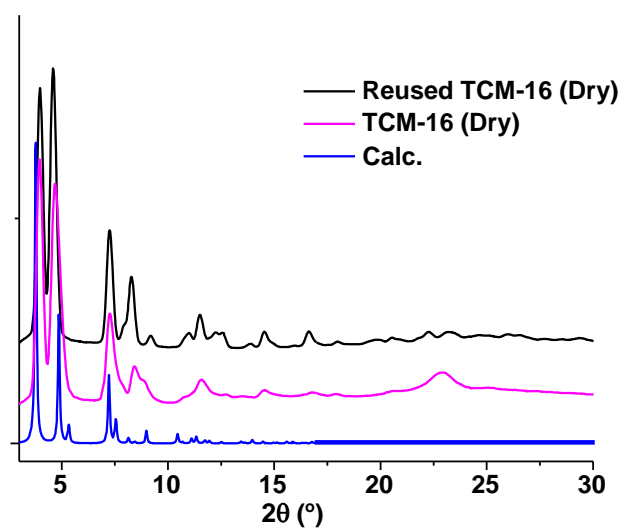


Figure S6: Experimental powder X-ray patterns of dried samples: i) reused, air-dried TCM-16, ii) pristine, air-dried TCM-16, and iii) calculated pattern (based on single-crystal data).

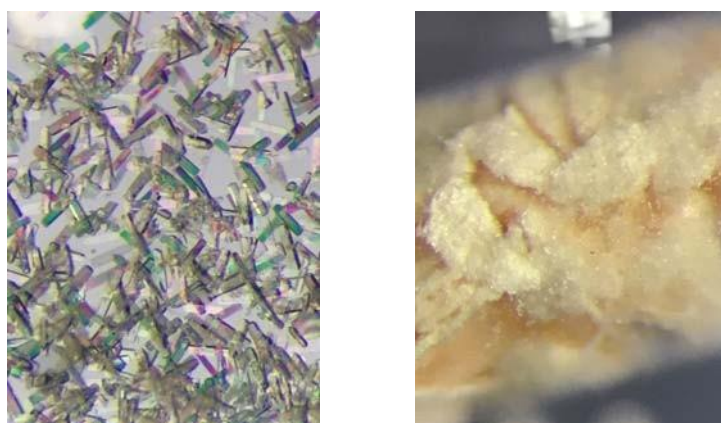


Figure S7: Optical micrographs of the morphology of TCM-16 crystals (*left*) and crystalline batch after the catalysis experiments (*right*, after 3 runs).

Table S2 provides selected examples of MOF-based catalysts that promote the cycloaddition reaction between CO₂ and epoxides.

Table S2: Some examples of MOFs that co-catalyse the cycloaddition between CO₂ and epoxides.

MOF	Organic linker ^a	Co-catalyst ^b	Substrate R =	Reaction conditions	Yield ^c
Hf-NU-1000 ^{S7}	H ₄ TBAPy	TBAB	-Ph	1 bar, 25 °C, 56 h	100 %
Ni-TCPE1 ^{S8}	TCPE	TBAB	-Ph	10 bar, 100 °C, 12 h	99 %
HKUST-1 ^{S9}	H ₃ BTC	--	-CH ₂ Cl	7 bar, 100 °C, 4 h	33 %
FJI-H7(Cu) ^{S10}	TBPP	TBAB	-CH ₂ Cl	1 bar, 25 °C, 60 h	66 %
MOF-5 ^{S11}	BDC	TBAB	-CH ₃	60 bar, 50 °C, 4 h	97 %
PCN-700-Me ₂ ^{S12}	Me ₂ -BPDC	TBAB	-Ph	1 bar, 50 °C, 10 h	93 %
PCN-700-Me ₂ ^{S12}	Me ₂ -BPDC	TBAB	-CH ₂ Cl	1 bar, 50 °C, 10 h	92 %
Zr(H ₄ L) ^{S13}	H ₈ L	TBAB	-Ph	10 bar, 100 °C, 12 h	95 %
Zr(H ₄ L) ^{S13}	H ₈ L	TBAB	-CH ₂ Cl	10 bar, 100 °C, 50 h	91 %
MOF-53 ^{S14}	bpH ₂ , bpyH ₂	DMAP	-CH ₂ Cl	16 bar, 100 °C, 2 h	80 %

^a: H₄TBAPy = 1,3,6,8-tetrakis(*p*-benzoic acid)pyrene; TCPE = tetrakis(4-carboxyphenyl)ethylene; H₃BTC = 1,3,5-benzenetricarboxylic acid; TBPP = 4',4''',4''''',4''''''-(porphyrin-5,10,15,20-tetray)tetrakis([1,1'-biphenyl]-4-carboxylic acid); BDC = benzene-1,4-dicarboxylate; Me₂-BPDC = 2,2'-dimethylbiphenyl-4,4'-dicarboxylate; H₈L = tetraphenylsilane tetrakis-4-phosphonic acid; bpH₂ = biphenyl-4,4'-dicarboxylic acid; bpyH₂ = 2,2'-bipyridine-5,5'-dicarboxylic acid.

^b: TBAB = tetrabutylammonium bromide; DMAP = 4-(dimethylamino)pyridine.

^c: Representative best results are listed herein.

S7. References

- [S1] R. K. Castellano and J. Rebek, Jr., *J. Am. Chem. Soc.*, 1998, **120**, 3657.
- [S2] Bruker. *SADABS*. 2001, Bruker AXS Inc., Madison, Wisconsin, USA.
- [S3] a) SHELXT: G. M. Sheldrick, *Acta Cryst.*, 2015, **A71**, 3-8; SHELXL: G. M. Sheldrick, (2015); b) *Acta Cryst.*, 2015, **C71**, 3-8.
- [S4] A. L. Spek, *Acta Cryst.*, 2009, **D65**, 148-155.
- [S5] V. A. Blatov, A. P. Shevchenko, D. M. Proserpio, *Cryst. Growth Des.* 2014, **14**, 7, 3576-3586.
- [S6] G. R. Fulmer, A. J. M. Miller, N. H. Sherden, H. E. Gottlieb, A. Nudelman, B. M. Stoltz, J. E. Bercaw, K. I. Goldberg, *Organometallics*, 2010, **29**, 2176-2179.
- [S7] C. Y. Gao, J. Ai, H. R. Tian, D. Wu, Z. M. Sun. *Chem. Commun.*, 2017, **53**, 1293-1296.
- [S8] S. Demir, S. Usta, H. Tamar, M. Ulusoy. *Microporous Mesoporous Mater.*, 2017, **244**, 251-257.
- [S9] J. Song, Z. Zhang, S. Hu, T. Wu, T. Jiang, B. Han. *Green Chem.*, 2009, **11**, 1031-1036.
- [S10] J. Zheng, M. Wu, F. Jiang, W. Su, M. Hong, *Chem. Sci.*, 2015, **6**, 3466-3470.
- [S11] C. Y. Gao, J. Ai, H. R. Tian, D. Wu, Z. M. Sun. *Chem. Commun.*, 2017, **53**, 1293-1296.
- [S12] S. Yuan, L. Zou, H. Li, Y. Chen, J. Qin, Q. Zhang, W. Lu, M. B. Hall, H. Zhou. *Angew. Chem. Int. Ed.*, 2016, **55**, 10776-10780.
- [S13] S. Demir, S. Usta, H. Tamar, M. Ulusoy. *Microporous Mesoporous Mater.*, 2017, **244**, 251-257.
- [S14] J. Song, Z. Zhang, S. Hu, T. Wu, T. Jiang, B. Han. *Green Chem.*, 2009, **11**, 1031-1036.